Electronic Supplementary Material (ESI) for RSC Advances.


**Dual step irradiation process for in situ generation and patterning of silver nanoparticles in a photocured film**

I. Roppolo, A. Doriguzzi Bozzo, M. Castellino, A. Chiappone, D. Perrone, K. Bejtka, S. Bocchini, M. Sangermano, A. Chiolerio

Electronic Supporting Infomation

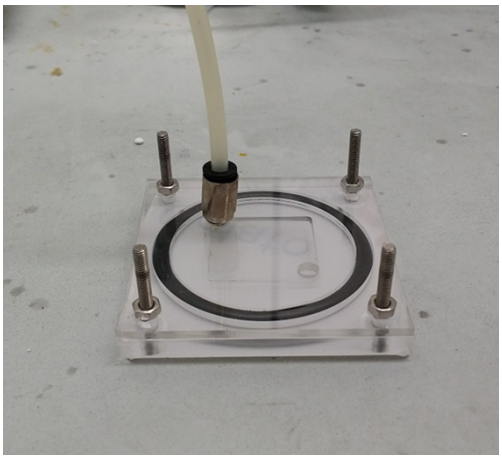

Figure S1 Lab-made device used for visible-induced photopolymerization experiments (size of the chamber used for placing the sample 1.5 x 1.5 cm x 0.2 cm)

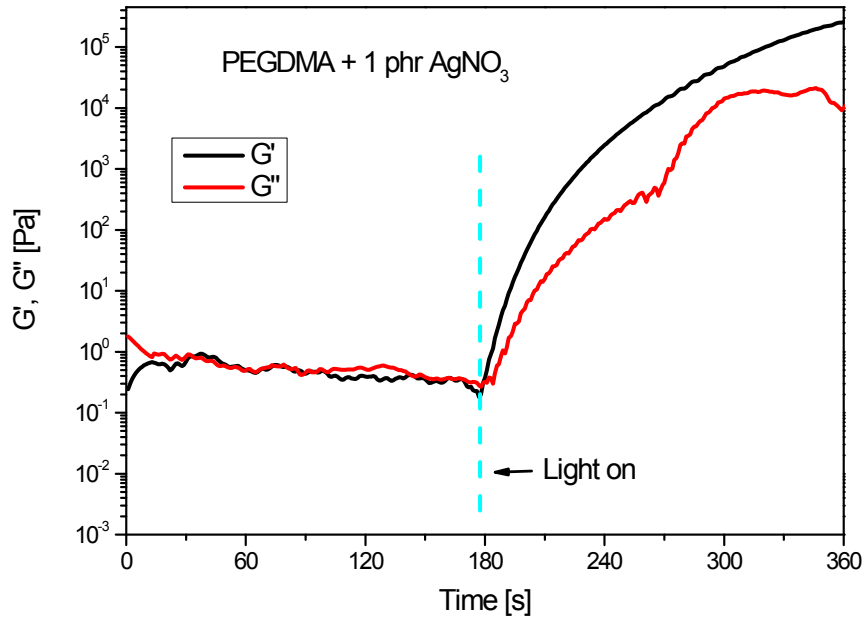


Figure S2 Time dependence of G' and G'' for sample PEGDMA + 1 Phr $AgNO_3$

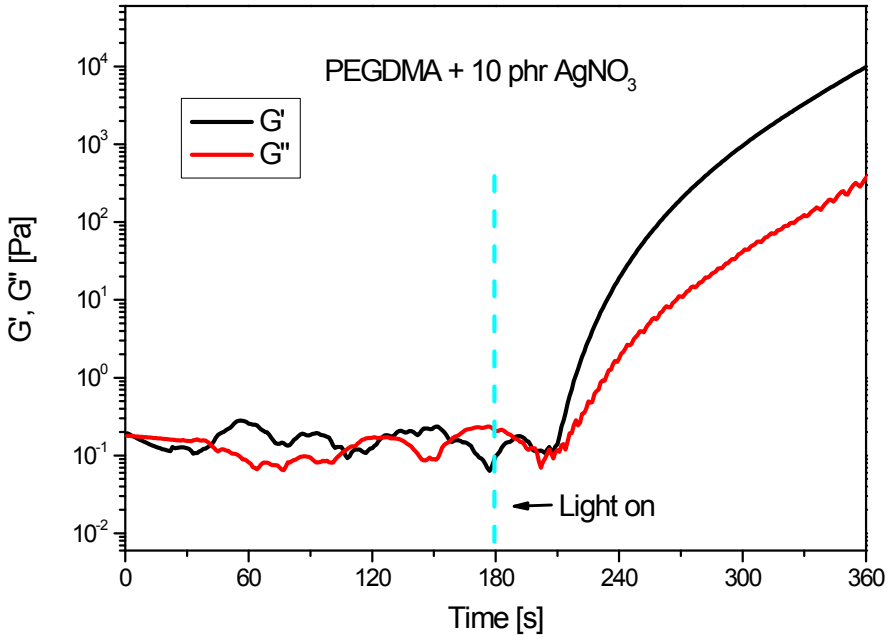


Figure S3 Time dependence of G' and G'' for sample PEGDMA + 5 Phr $AgNO_3$

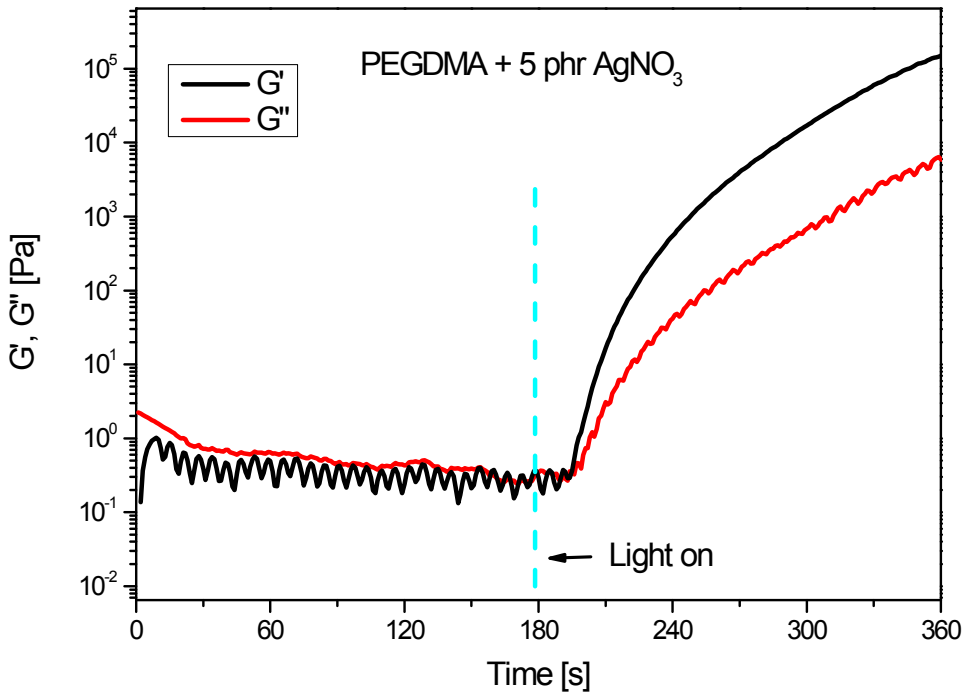


Figure S4 Time dependence of G’ and G’’ for sample PEGDMA + 10 Phr $AgNO_3$

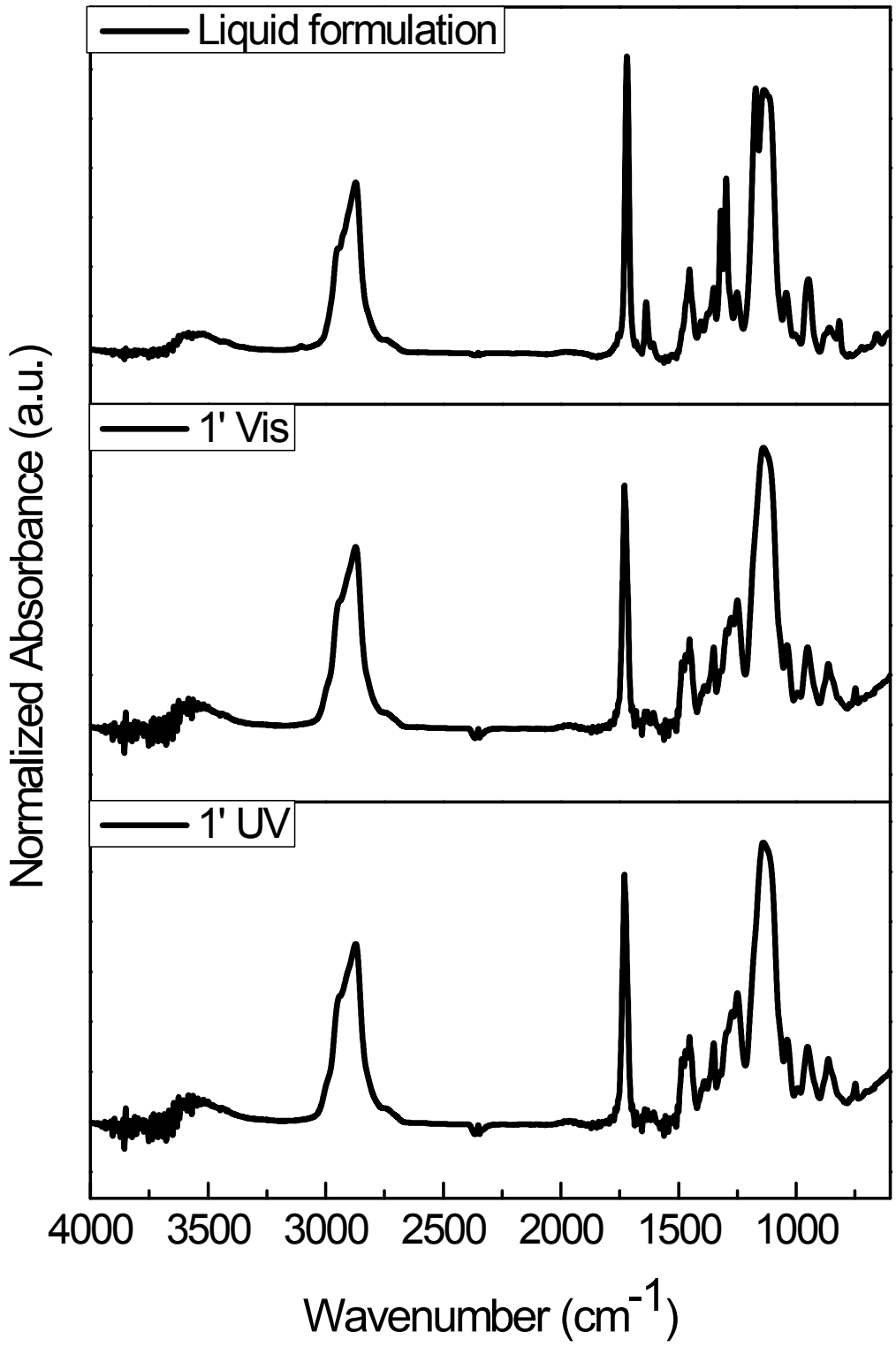


Figure S5 FT-IR for sample PEGDMA

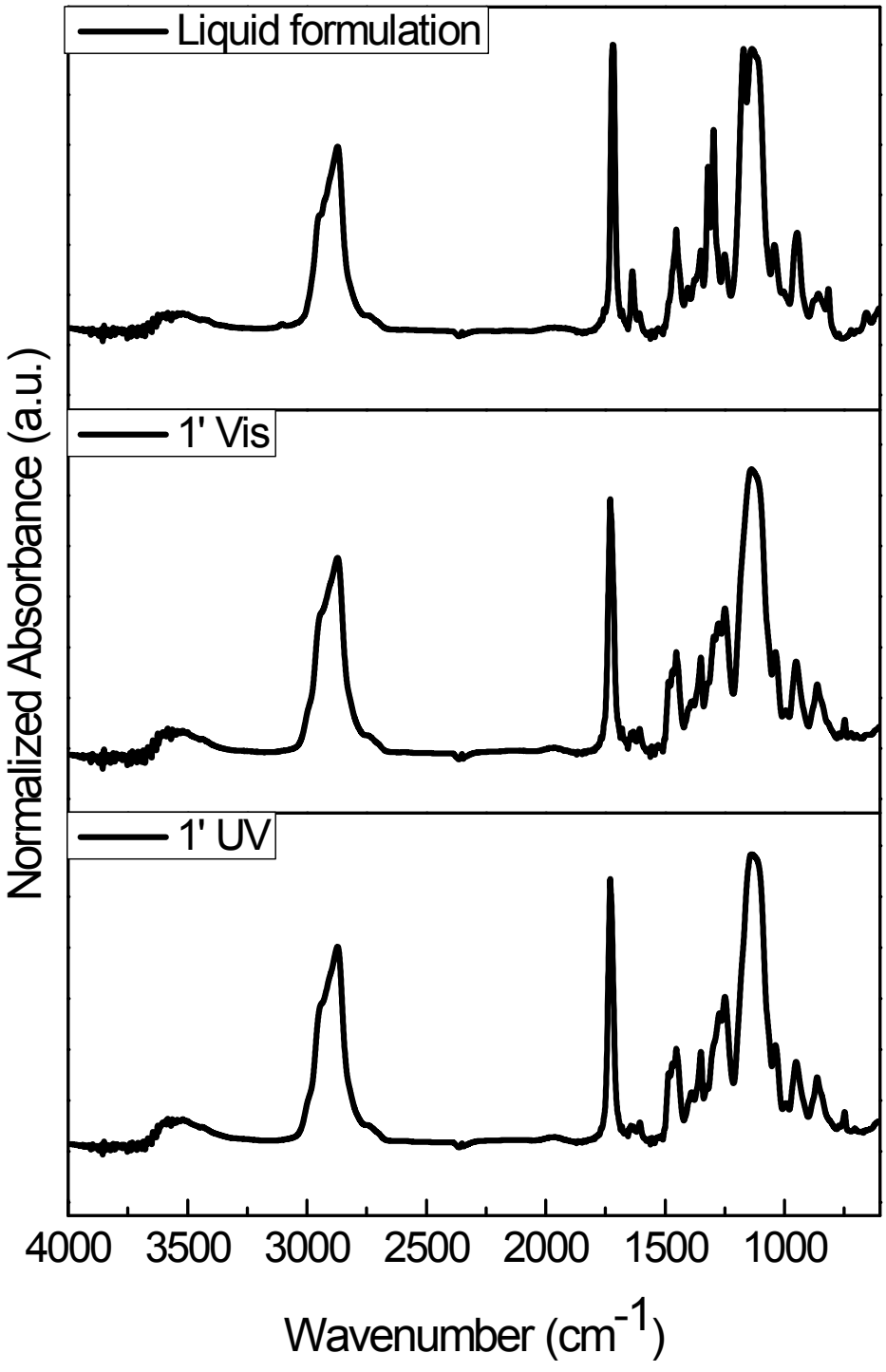


Figure S6 FT-IR for sample PEGDMA + 1 phr $AgNO_3$

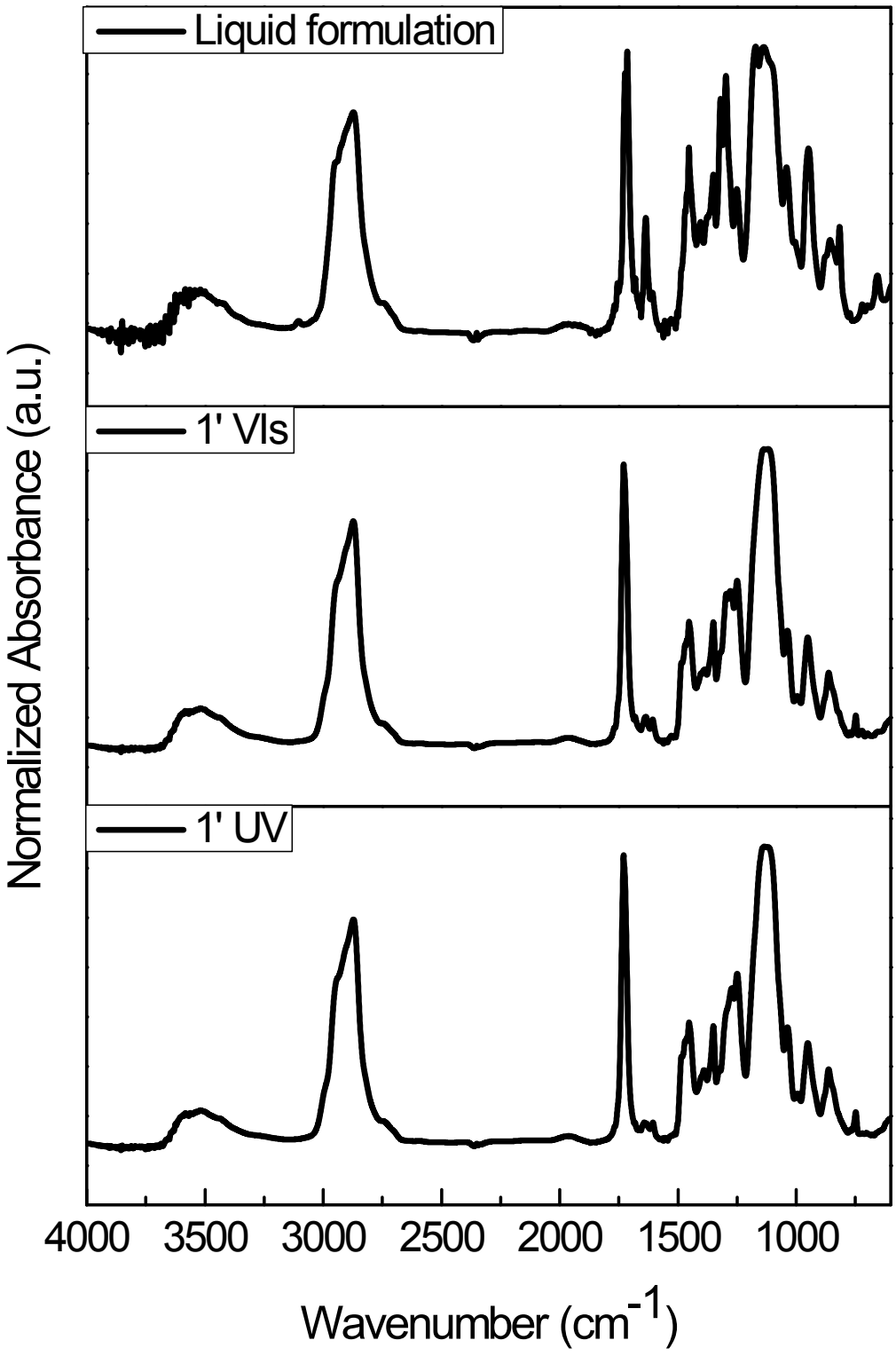


Figure S7 FT-IR for sample PEGDMA + 5 phr $AgNO_3$

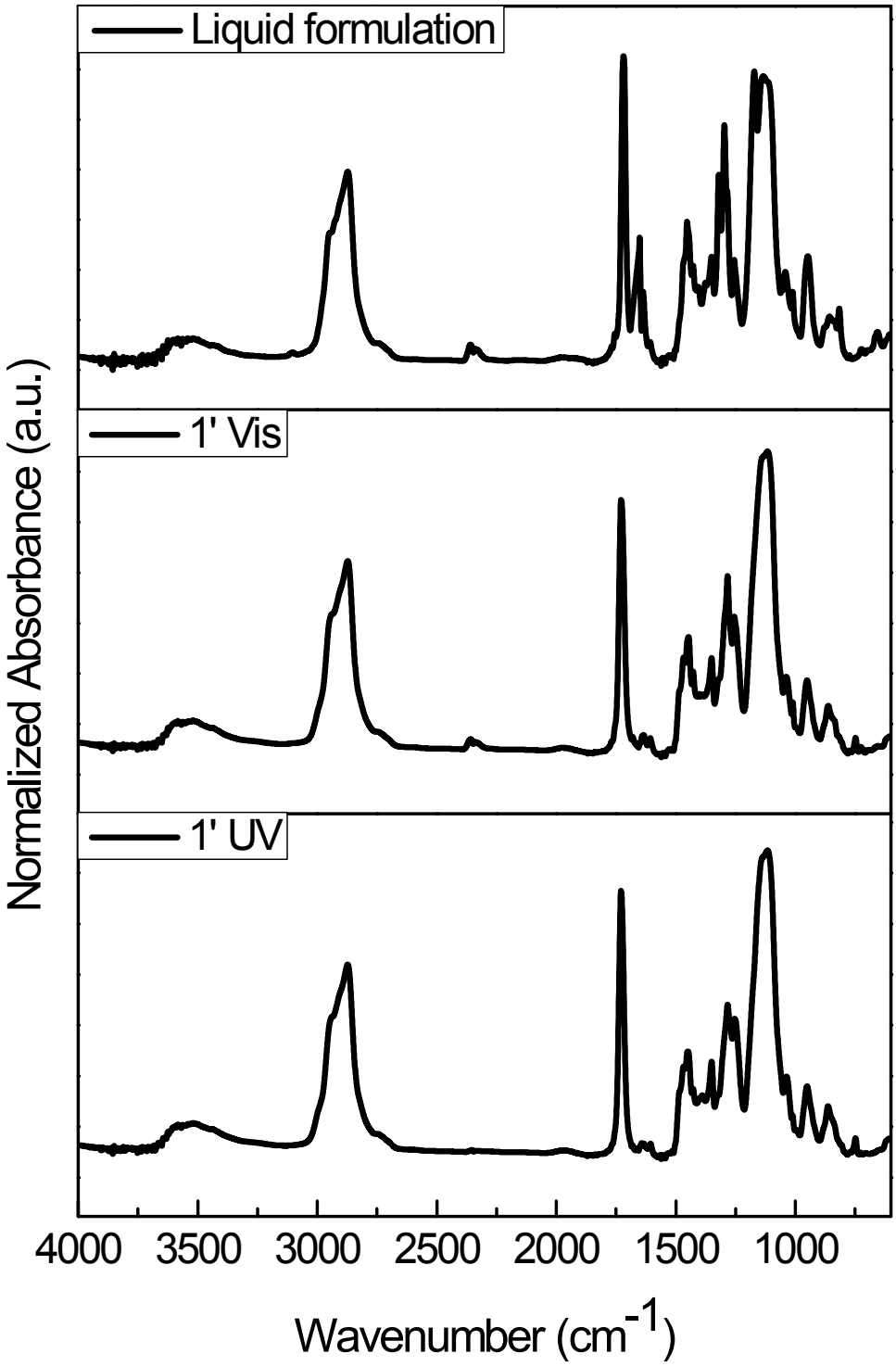


Figure S8 FT-IR for sample PEGDMA + 10 phr $AgNO_3$

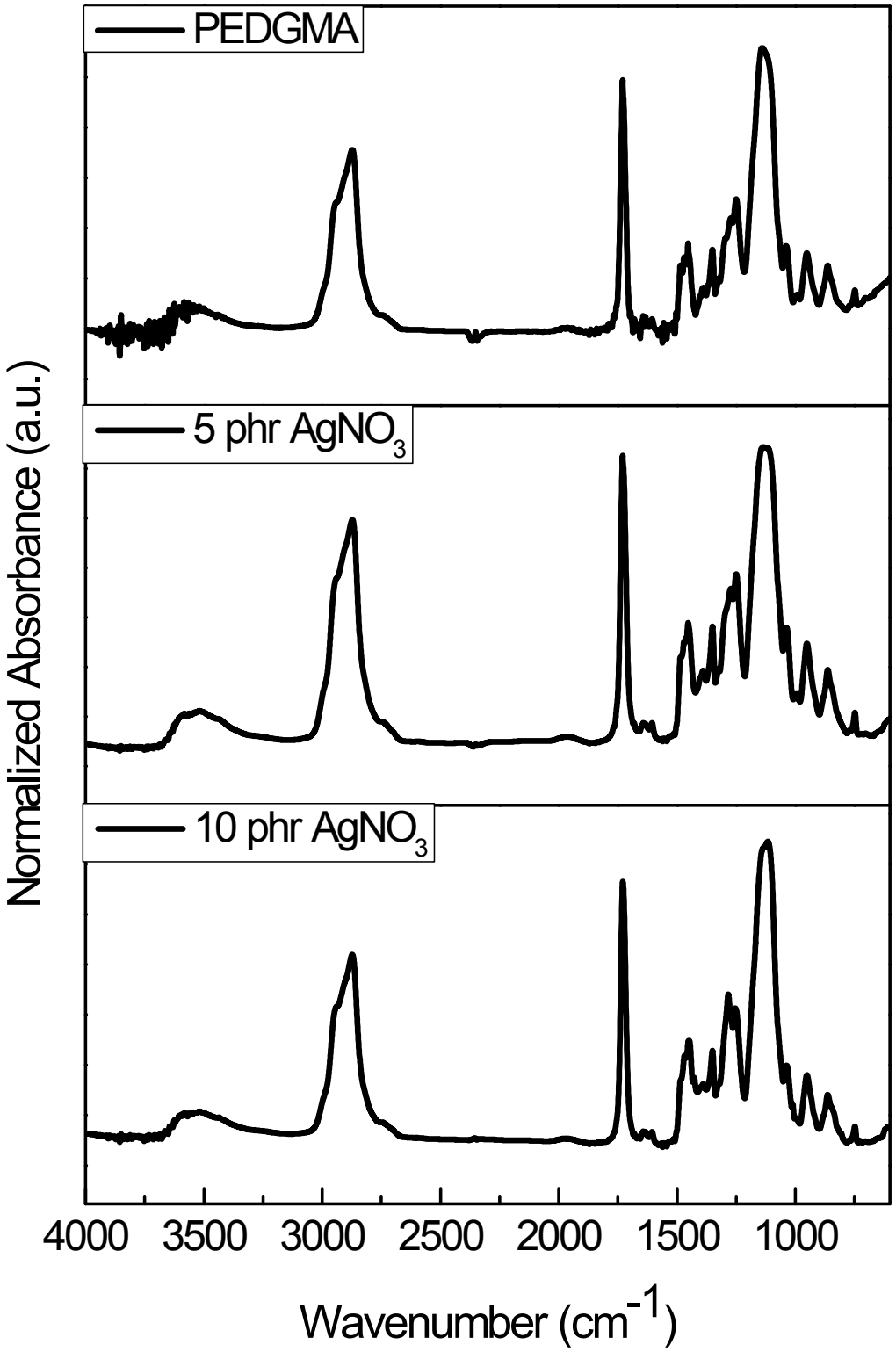


Figure S9 FT-IR for samples PEGDMA, PEGDMA + 5 phr $AgNO_3$ and PEGDMA + 10 phr $AgNO_3$ after UV irradiation

The FT-IR spectrum for the PEGDMA/photoinitiators system shows only the absorbances of the starting monomer (Table T1). The methacrylic $=CH_2$ originates the aromatic stretching at 3105 $cm^{-1}$ [1] and the C-H distortion at 817 $cm^{-1}$ [7]. Between 3000 and 2700 $cm^{-1}$ the C-H stretchings of aliphatic CH, $CH_2$ and $CH_3$ are present [2] while $CH_3$ distortion is present at 1455 $cm^{-1}$ [4]. The methacrylate system –C=C-COO- originates different absorbances due to C=O stretching at 1720 $cm^{-1}$ [3], C=C stretching at 1638 $cm^{-1}$ [3] and the asymmetric/symmetric C-O-C stretching [5] respectively at 1320/1296 and 1173 $cm^{-1}$. Finally the C-O-C asymmetric stretching of ether group is visible at 1134 $cm^{-1}$ [6]. After irradiation with visible light the methacrylic group absorbances disappears, the C=O stretching shift at 1729 $cm^{-1}$ while the other absorbances are located exactly at the same wavenumber. There are no further modification in absorbance after UV irradiation. The samples with different content of $AgNO_3$ have spectra that are practically superimposable with their homologous.

Table T1. FT-IR Band Assignment of PEGDMA sample

| PEGDMA | | PEGDMA after Vis irradiation | | PEGDMA after UV irradiation | |
|---|---|---|---|---|---|
| Assignment | $cm^{-1}$ | Assignment | $cm^{-1}$ | Assignment | $cm^{-1}$ |
| $\nu_{C\text{-}H\ arom}$ | 3105 [1] | | | | |
| $\nu_{CH/CH2/CH3}$ aliphatic | 3000-2700 [2] | $\nu_{CH/CH2/CH3}$ aliphatic | 3000-2700 [2] | $\nu_{CH/CH2/CH3}$ aliphatic | 3000-2700 [2] |
| $\nu_{C=O}$ methacrylate | 1720 [3] | $\nu_{C=O}$ ester | 1729 [3] | $\nu_{C=O}$ ester | 1729 [3] |
| $\nu_{C=C}$ methacrylate | 1638 [3] | | | | |
| $\delta_{asCH3}$ | 1455 [4] | $\delta_{asCH3}$ | 1455 [4] | $\delta_{asCH3}$ | 1455 [4] |
| $\nu_{asC\text{-}O\text{-}C}$ methacrylate | 1320/1296 [5] | | | | |
| $\nu_{sC\text{-}O\text{-}C}$ methacrylate | 1173 [5] | | | | |
| $\nu_{asC\text{-}O\text{-}C}$ ether | 1134 [6] | $\nu_{asC\text{-}O\text{-}C}$ ether | 1134 [6] | $\nu_{asC\text{-}O\text{-}C}$ ether | 1134 [6] |
| $\delta_{=CH2}$ methacrylate | 817 [7] | | | | |

[1] Socrates, George Infrared and Raman characteristic group frequencies: tables and charts. John Wiley & Sons, 2004 Table 3.2 Alkene C- H vibrations p.73.

[2] Socrates, George Infrared and Raman characteristic group frequencies: tables and charts. John Wiley & Sons, 2004 Table 2.1 Alkane C-H stretching vibrations for alkane functional groups as part of a residual saturated hydrocarbon portion of the molecule p.51.
[3] Socrates, George Infrared and Raman characteristic group frequencies: tables and charts. John Wiley & Sons, 2004 Table 10.19 Ester, haloformate, and carbonate c=o stretching vibrations p.136.
[4] Socrates, George Infrared and Raman characteristic group frequencies: tables and charts. John Wiley & Sons, 2004 Table 2.2 Alkane C-H deformation vibrations for alkane functional groups as part of a residual saturated hydrocarbon portion of molecule p.52.
[5] Socrates, George Infrared and Raman characteristic group frequencies: tables and charts. John Wiley & Sons, 2004 Table 10.20 Ester, haloformate, and carbonate C-O-C stretching vibrations p.138.
[6] Socrates, George Infrared and Raman characteristic group frequencies: tables and charts. John Wiley & Sons, 2004 Table 7.1 Ether C-O stretching vibrations p.102.
[7] Socrates, George Infrared and Raman characteristic group frequencies: tables and charts. John Wiley & Sons, 2004 p.141.

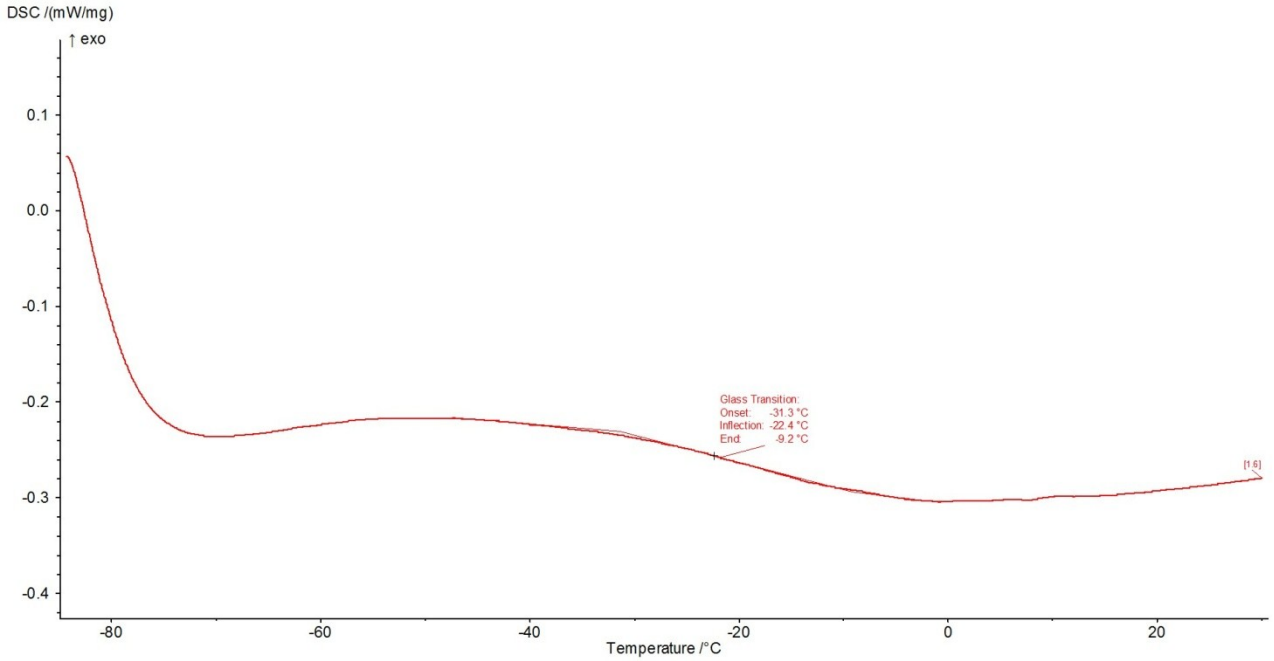


Figure S10 DSC curve for sample PEGDMA after visible irradiation

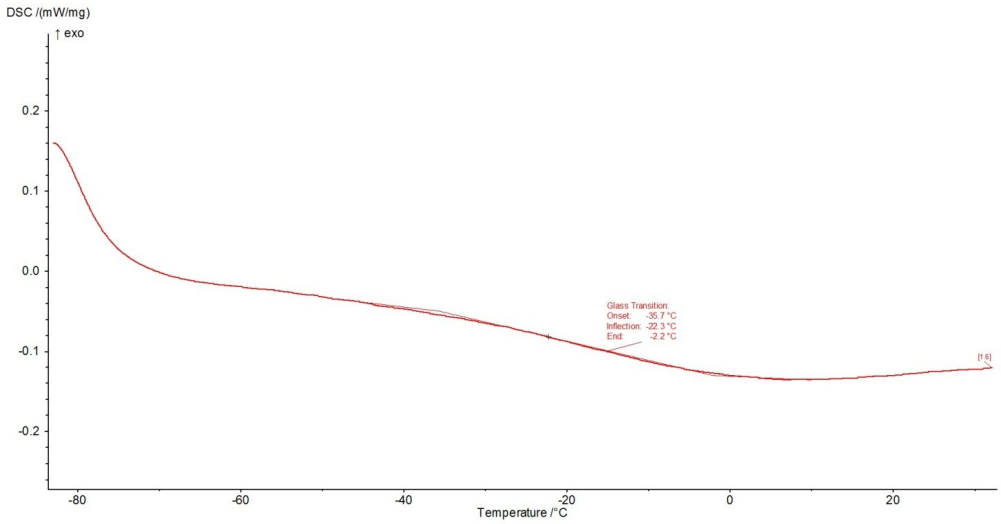


Figure S11 DSC curve for sample PEGDMA after UV irradiation

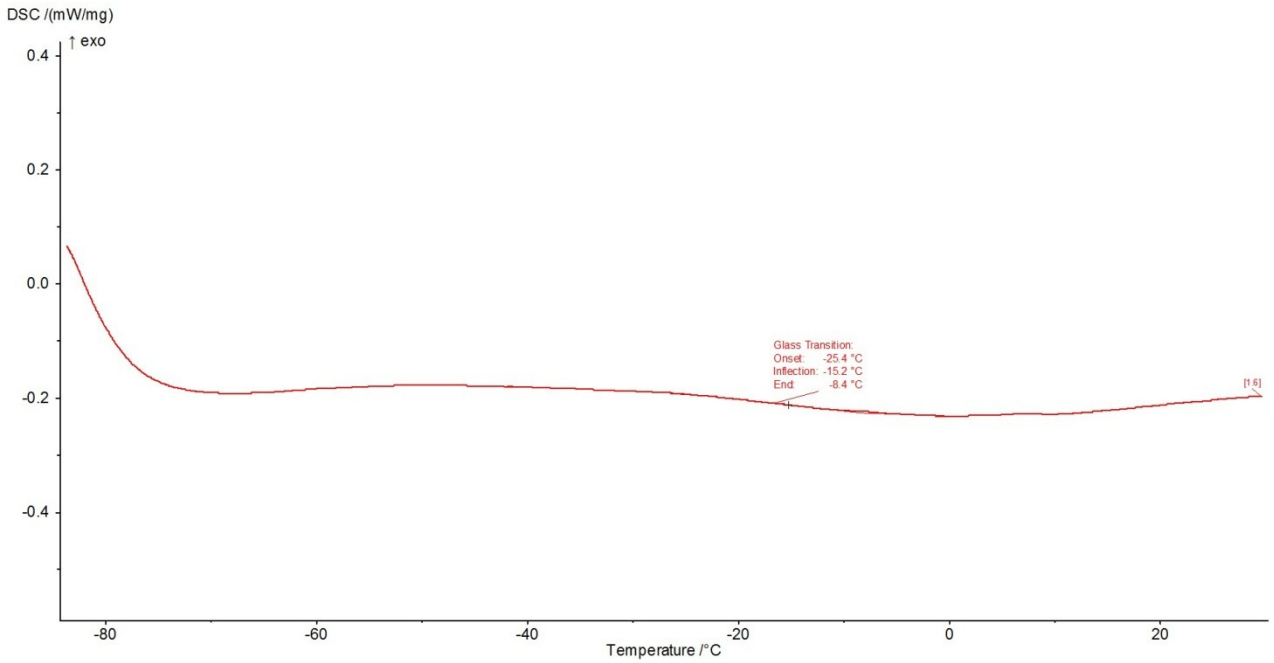


Figure S12 DSC curve for sample PEGDMA + 1 phr $AgNO_3$ after UV irradiation

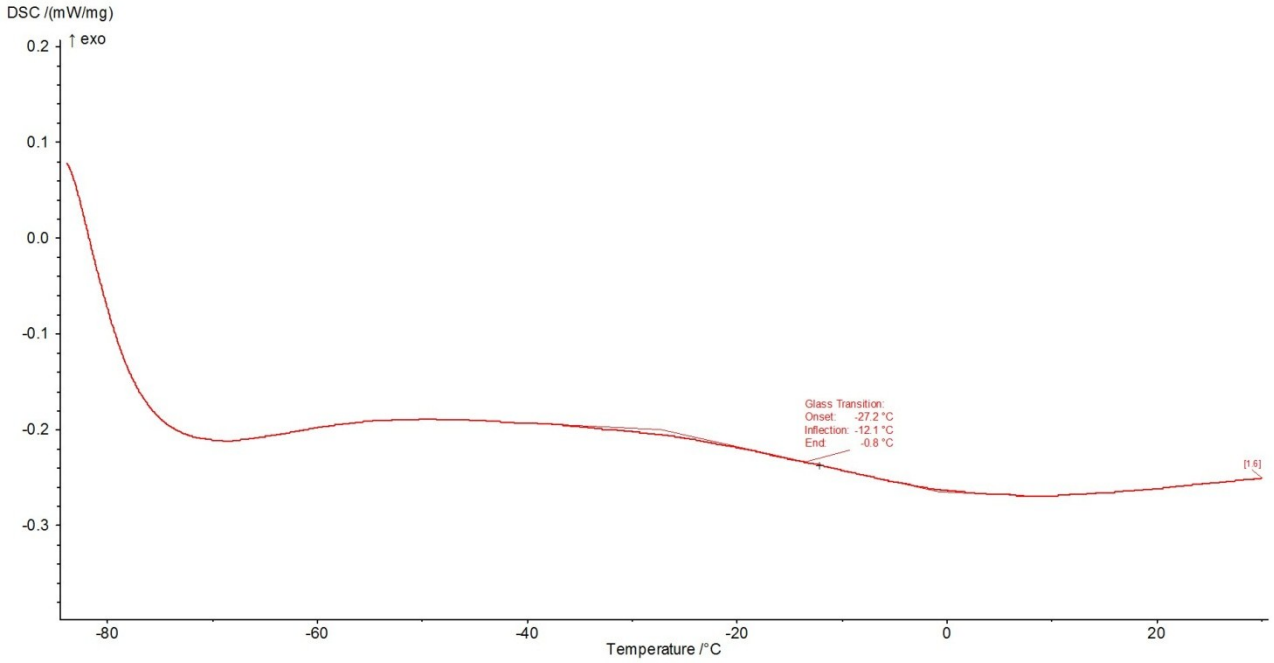


Figure S13 DSC curve for sample PEGDMA + 5 phr $AgNO_3$ after UV irradiation

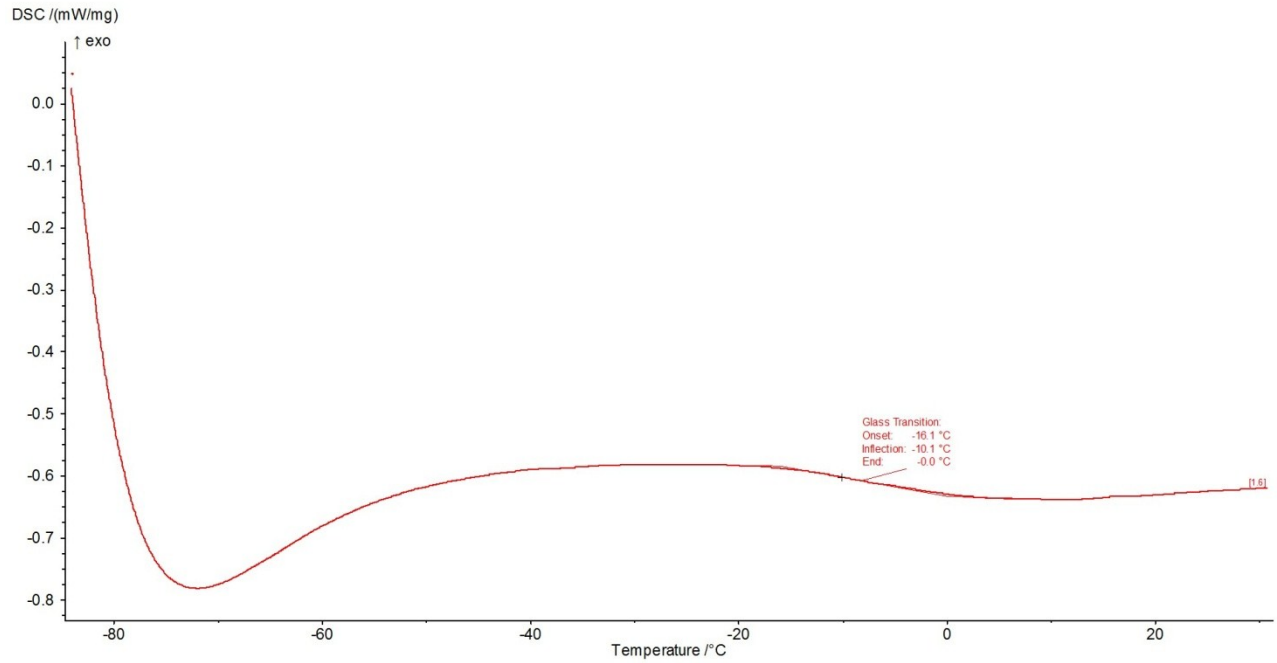


Figure S14 DSC curve for sample PEGDMA + 10 phr $AgNO_3$ after UV irradiation

**Plasmon of resonance analysis**

The plasmon of resonance evidenced in the UV-Vis spectra collected at different irradiation times was analyzed by means of single Gaussian fit and triple Gaussian fits. In Table T2 the most important parameters extrapolated from the single fits are reported.

Table T2 Parameters extrapolated from single Gaussian fit of the plasmons of resonance

| Irradiation Time (s) | Amplitude (a.u.) | $\lambda_{MAX}$ (nm) | FWHM | $R^2$ |
|---|---|---|---|---|
| 30 | 0.0225 | 432 | 235.4 | 0.99681 |
| 60 | 0.0308 | 420 | 249.3 | 0.99702 |
| 120 | 0.0402 | 405 | 284.5 | 0.99802 |
| 300 | 0.0476 | 407 | 286.2 | 0.99542 |
| 600 | 0.0502 | 420 | 262.1 | 0.99711 |
| 1800 | 0.197 | 442 | 143.8 | 0.99822 |
| 3600 | 0.472 | 441 | 119.8 | 0.99944 |

It is possible to evidence different facts:

- The amplitude of the peak (height) increases increasing the irradiation time, this could be correlated to an increase of the concentration of Ag NPs in the polymeric network (higher number and shorter interdistance);
- The maximum of the Gauss curve first shifts toward lower wavelengths and then increases to higher wavelengths (after 120 s irradiation time) finally reaching a plateau around 440 nm. Since the maximum could be related to the diameter of the NPs, it is possible to say that with the irradiation, small NPs first nucleate, red-shifting the maximum of the fitting curve. Then they start to coalesce, generating thus bigger NPs and blue-shifting the $\lambda_{MAX}$;
- The FWHM first increases and then decreases, following a trend similar to the $\lambda_{MAX}$, this could be explained considering a broadening of the peak during the initial generation of Ag small clusters, indicating that a broad range of NPs of different dimensions are generated and are growing. For longer irradiation times the material reaches an equilibrium, with narrower NPs distribution.

However, considering that the generation kinetics of Ag NPs is a very complex mechanism and it is possible to envisage that different families of Ag NPs are generated during the irradiation, a triple Gaussian fit was performed in order to better describe the resonance plasmon. The results are reported in the following graphs (Figures S14-S18)

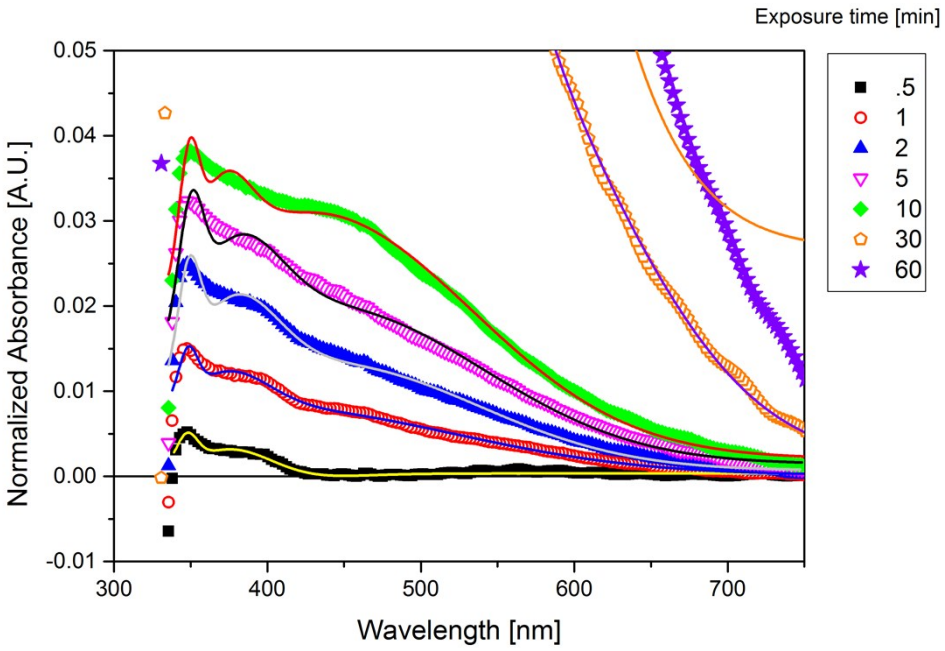


Figure S15 3- Gaussian curves Fit of Plasmon of resonance for 30 s- 600 s UV irradiation time

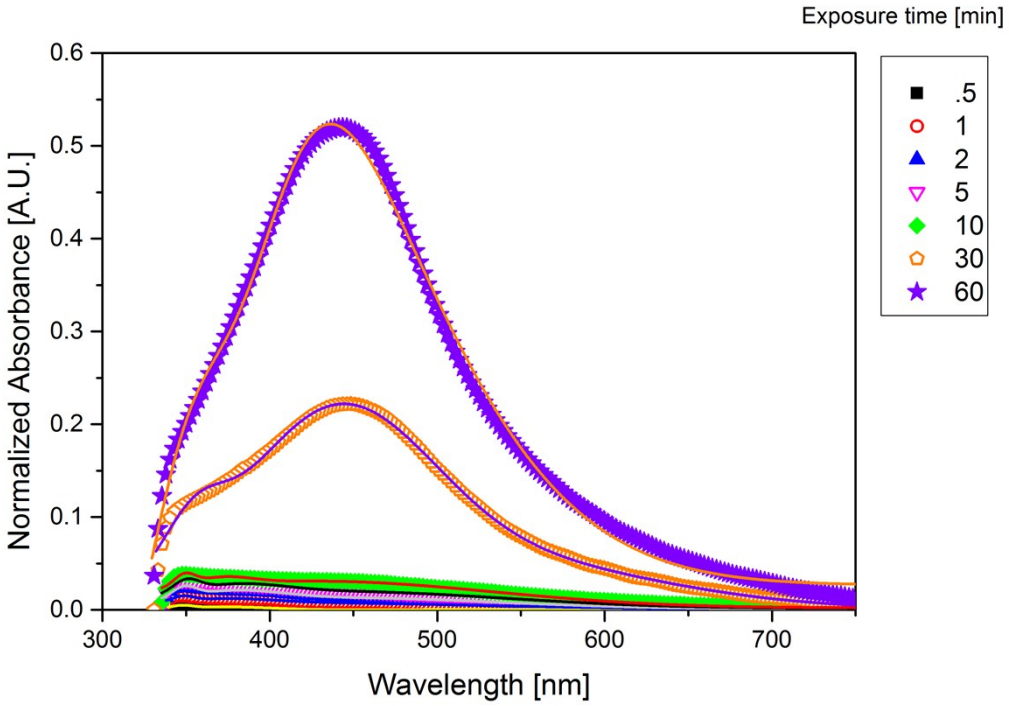


Figure S16 3- Gaussian curves Fit of Plasmon of resonance for 1800 s- 3600 s UV irradiation time

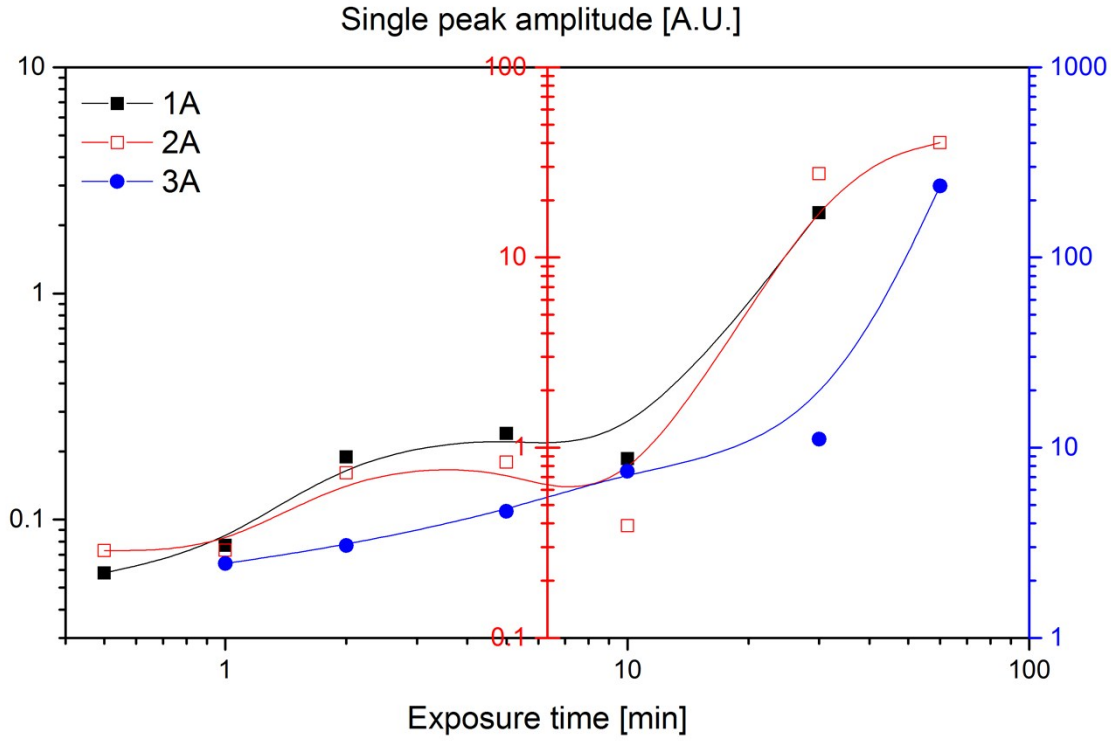


Figure S17 Amplitude (height) of the three Gaussian functions (1, 2 and 3) used to fit UV-Vis spectra; each ordinate axis in color corresponds to its Gaussian function accordingly;

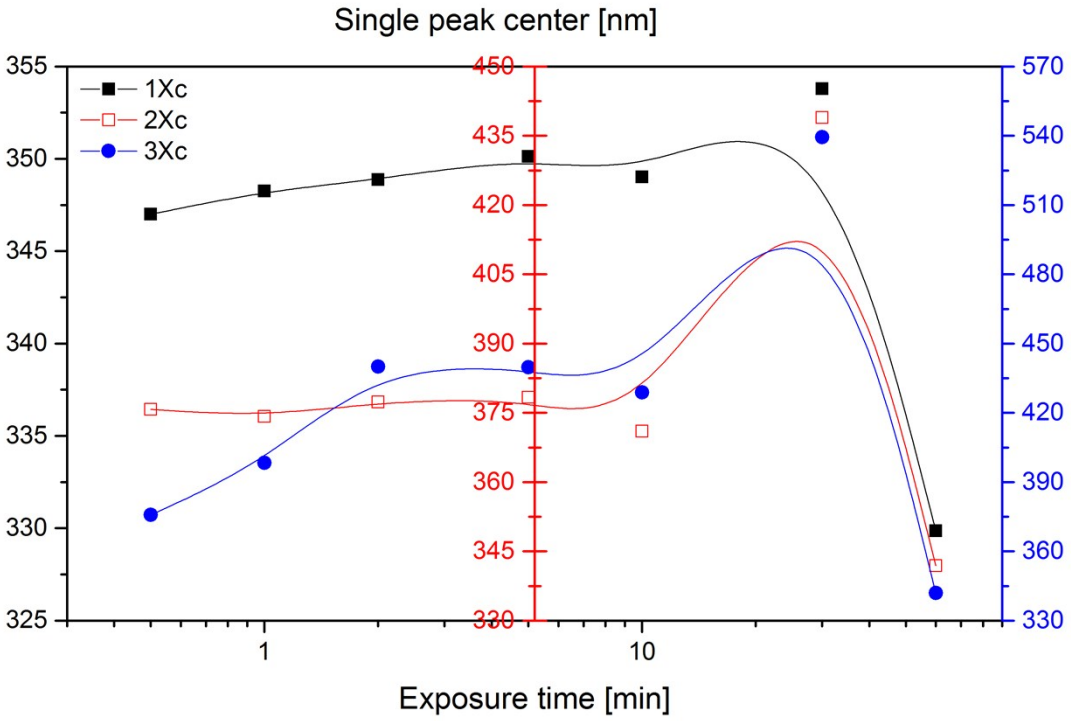


Figure S18 $\lambda_{MAX}$ of the fitted Gaussian curves

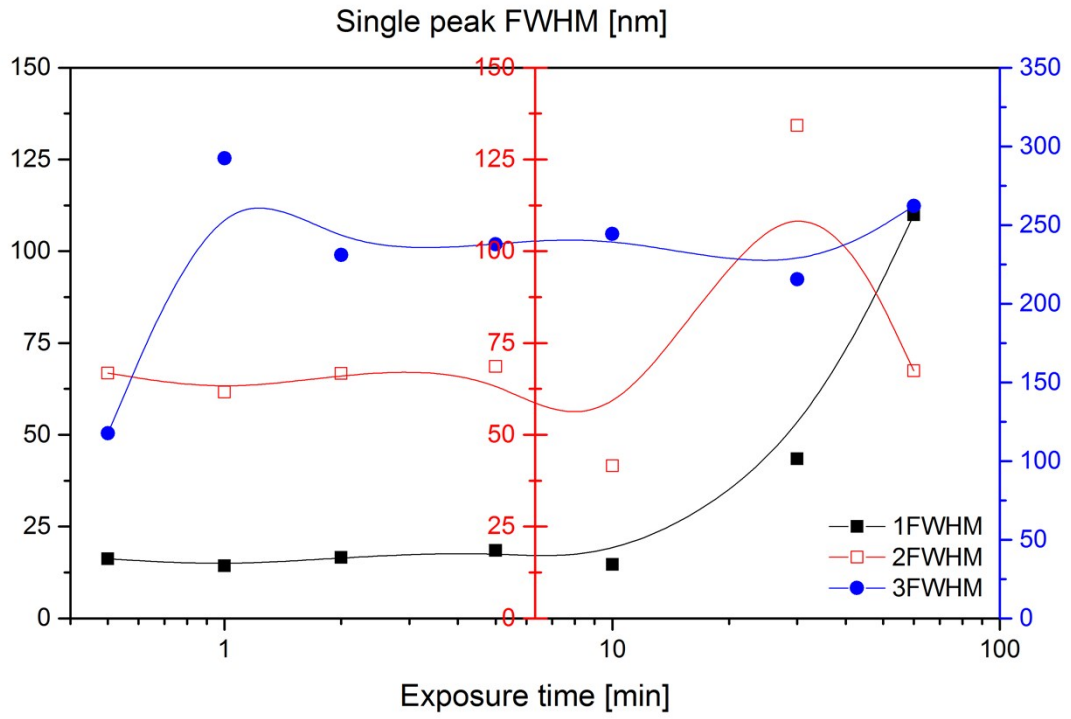


Figure S19 FWHM of the fitted Gaussian curves

The graphs suggest that a 3 curves model well describes the UV-Vis spectra. They evidence the presence of a small- diameter family of NPs (curve centered around 345 nm) that is prevalent in the early stages of the irradiation: increasing the irradiation time first a second family (centered around 375 nm) and then a third family (centered around 445 nm) appear, indicating the increase of the NPs dimension. This is in good agreement with the discussion above reported. A clear two-stage process is less evident from this analysis, the only clear difference in trend is represented by samples irradiated for longer times (30 and 60 min), whose properties are quite different from the other samples.

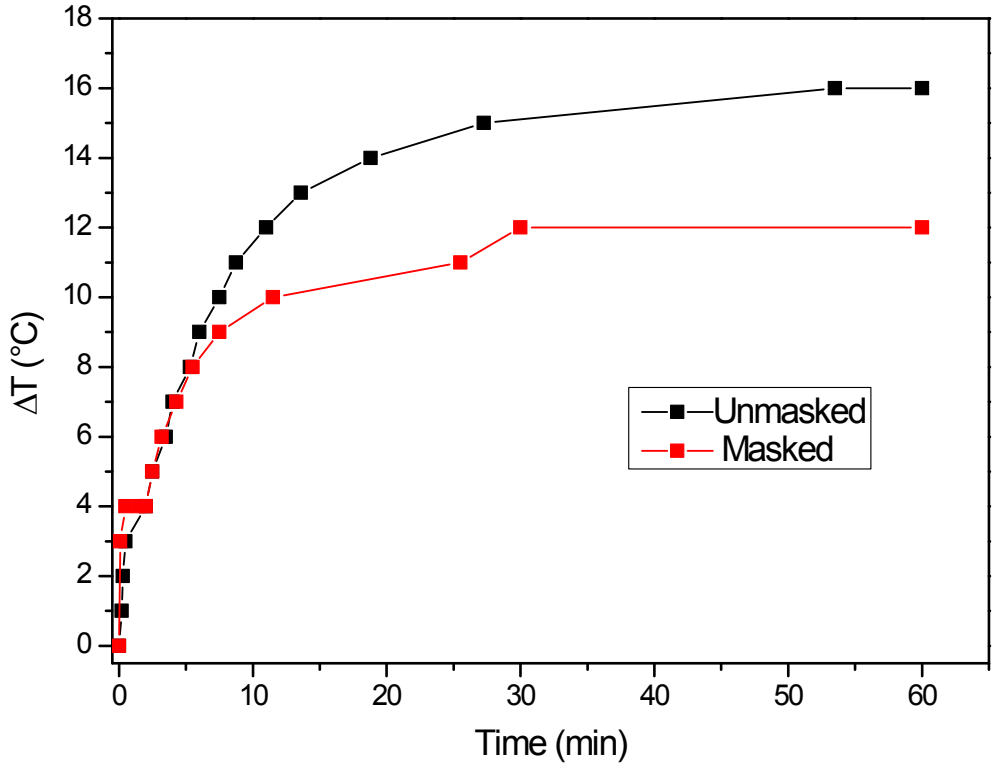


Figure S20 Temperature increase in the film during UV irradiation with and without mask

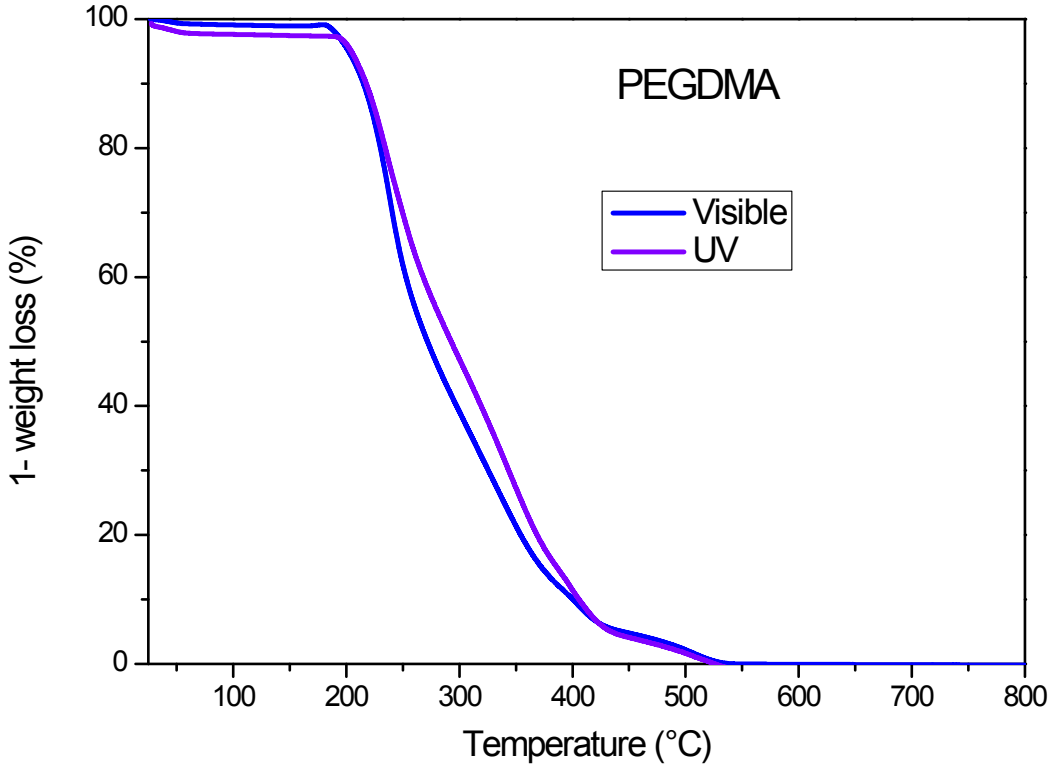


Figure S21 TGA curve of PEGDMA

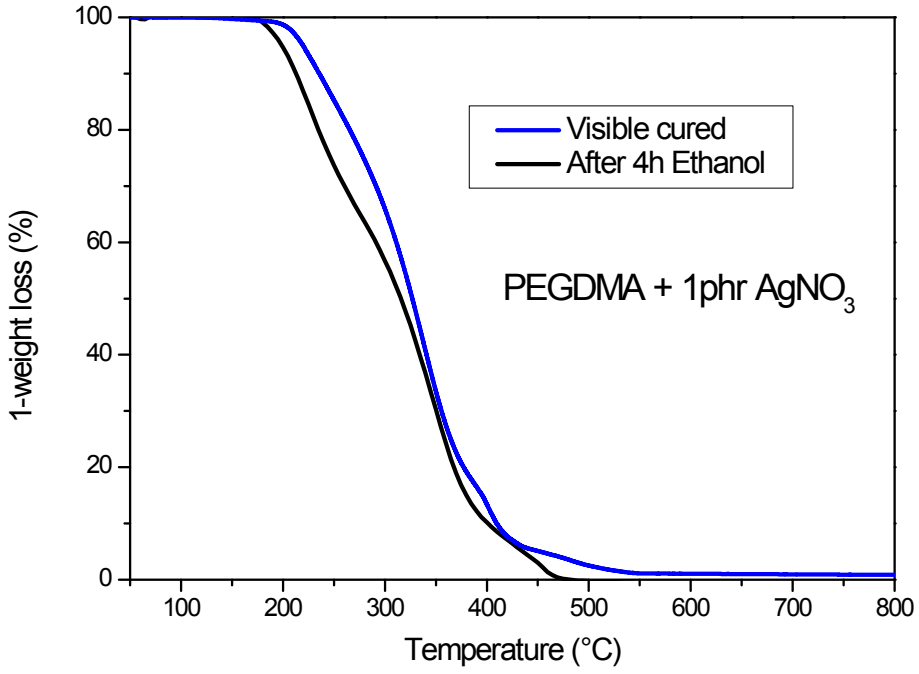


Figure S22 TGA curve of PEGDMA + 1phr $AgNO_3$

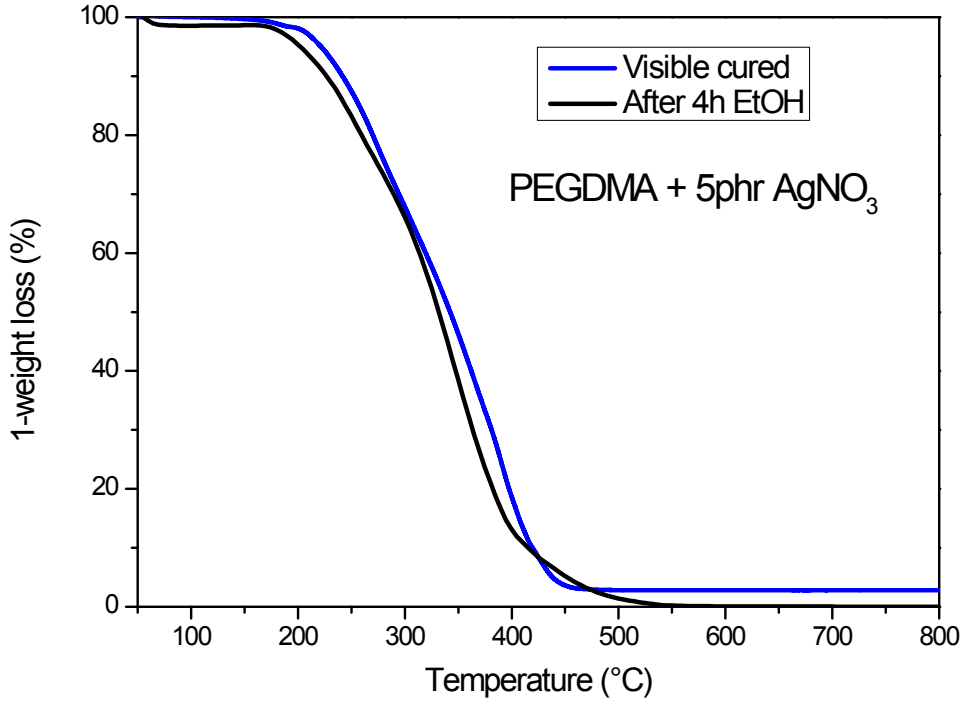


Figure S23 TGA curve of PEGDMA + 5 phr $AgNO_3$

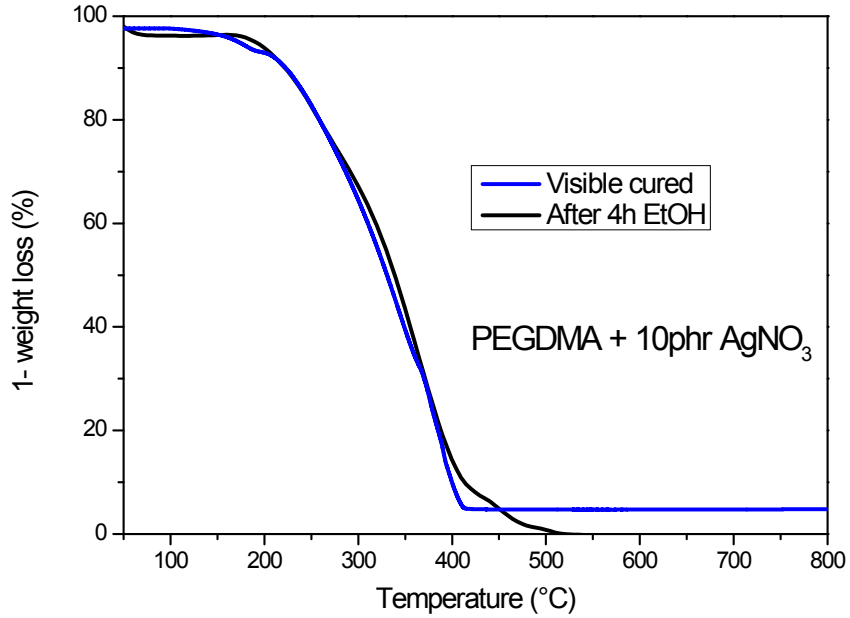


Figure S24 TGA curve of PEGDMA + 10 phr $AgNO_3$

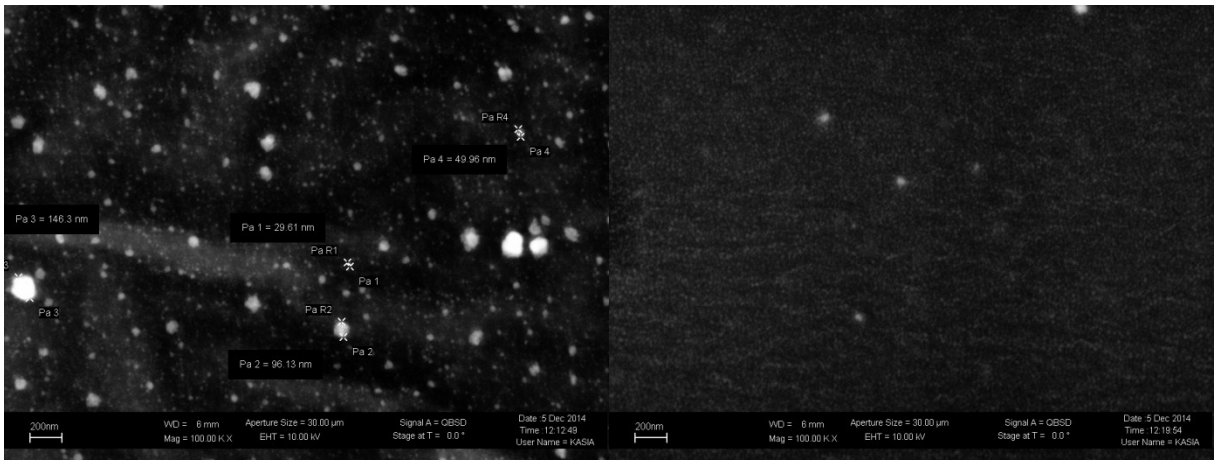


Figure S25 Magnification of Figure 6a: top (left) and bottom (right) part of the cross section of PEGDMA + 5 phr $AgNO_3$ after 10 minutes of UV irradiation: few NPS are present in the upper part while the rest is almost neat.

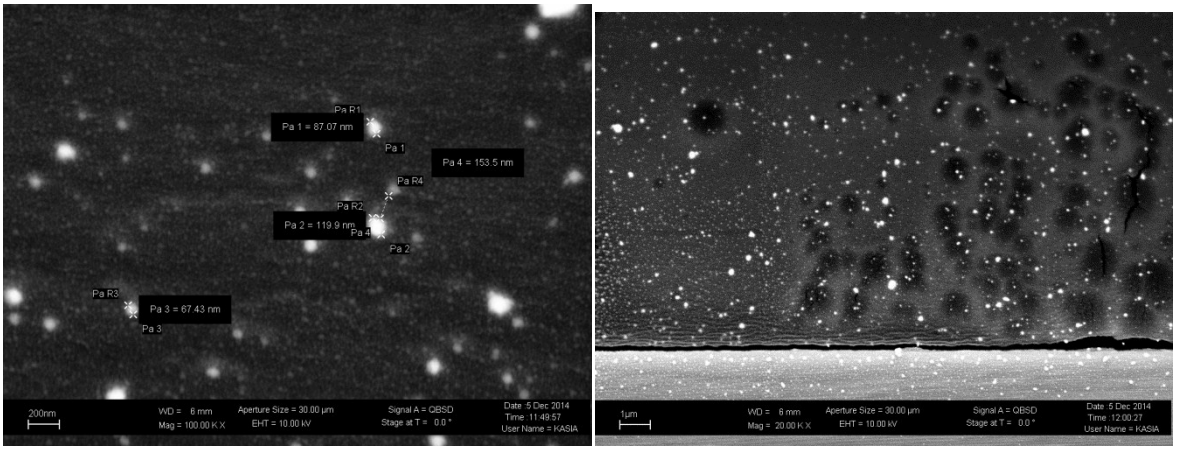


Figure S26 Magnification of Figure 6b: top (left) and bottom (right) part of the cross section of PEGDMA + 5 phr $AgNO_3$ after 30 minutes of UV irradiation: NPs are present almost homogeneously all along the polymeric matrix.

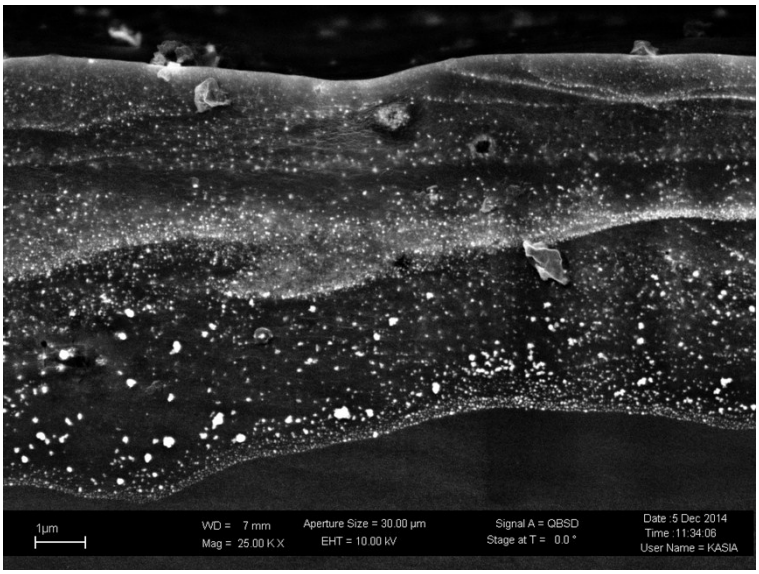


Figure S27 Magnification of Figure 6c: top part of the cross section of PEGDMA + 5 phr $AgNO_3$ after 60 minutes of UV irradiation: NPs are present confined in this region inducing the silver mirror like aspect..

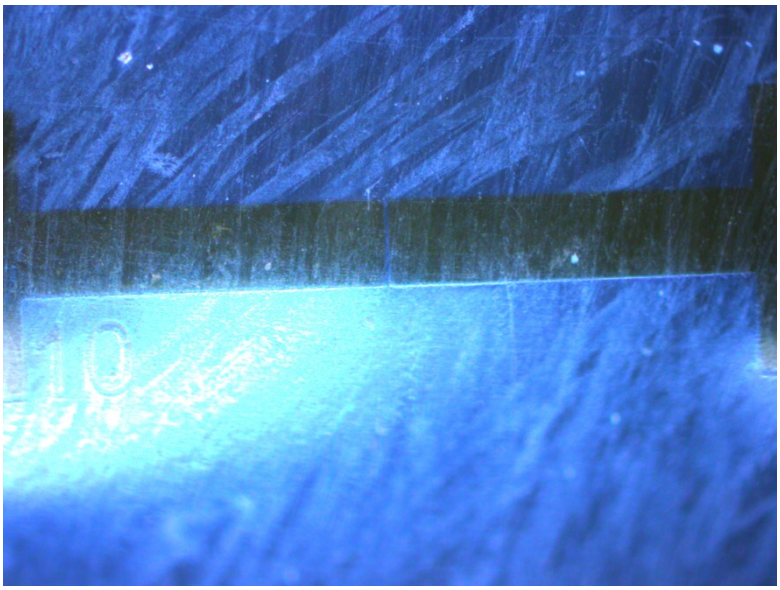

Figure S28 Optical microscope image of a 10 µm gap patterned in PEGDMA + 5 phr $AgNO_3$ sample

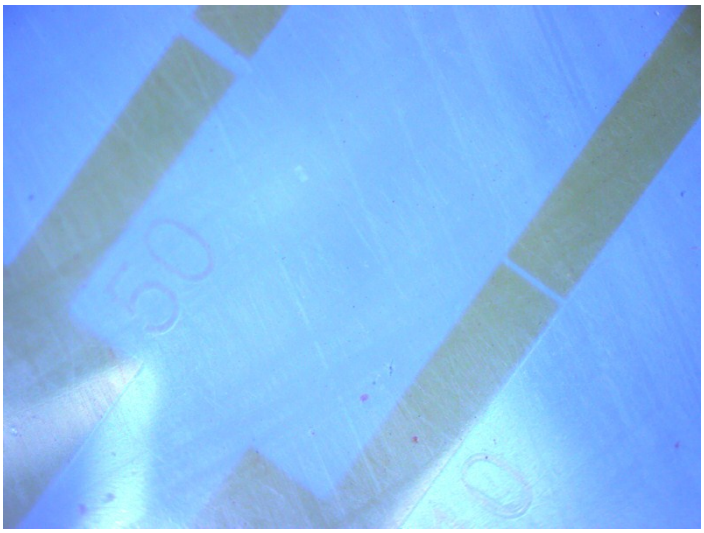


Figure S29 Optical microscope image of different structures patterned in PEGDMA + 5 phr $AgNO_3$ sample

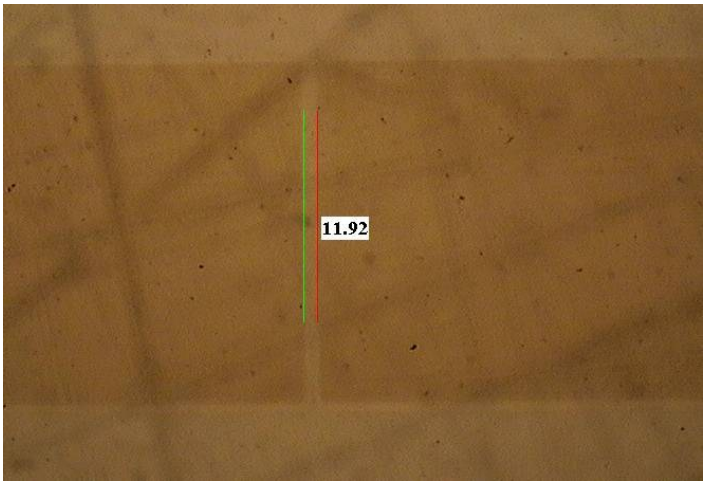


Figure S30 Optical microscope image of a 10 μm gap patterned in PEGDMA + 5 phr $AgNO_3$ sample, measurement of the patterned gap


Figure S31 Free standing film in which different electrode-like structures were patterned

Figure S32 Picture of the same sample just after patterning/washing procedure (left) and after 6 months at room conditions.